Proceedings of the 2018 Bath/ASME Symposium on Fluid Power and Motion Control
FPMC2018
September 12-14, 2018, University of Bath, Bath, United Kingdom

FPMC2018-8834

CALCULATING THE MECHANICAL AND VOLUMETRIC EFFICIENCIES FOR CHECK-VALVE TYPE, DIGITAL DISPLACEMENT PUMPS

Noah Manring
Mechanical and Aerospace Engineering
University of Missouri
Columbia, Missouri 65211
573-882-0693, ManringN@missouri.edu

Christopher Williamson
Danfoss Power Solutions
Ames, Iowa 50010, USA
515-956-5611, cwilliamson@danfoss.com

ABSTRACT

Methods for calculating the volumetric and mechanical efficiencies for hydrostatic pumps and motors are well known, and depend upon the precise volumetric displacement of the machine. It is also known that check-valve type, digital displacement pumps undergo an apparent reduction in volumetric displacement as pressures increase, and that this reduction in displacement is realized at both the input and output terminals of the machine. Recent work has been conducted to physically explain and quantify this apparent reduction in the volumetric displacement. In this present paper, the results of this previous work are used to calculate and plot the volumetric and mechanical efficiencies of a digital displacement pump, using measured values of pump efficiency and fluid bulk modulus. It is shown that without accounting for the apparent reduction in volumetric displacement, the volumetric and mechanical efficiency calculations may produce unrealistic results, and be in error by as much as 7%.

NOMENCLATURE

N	number of pistons within the pump
P	instantaneous fluid pressure within a single piston chamber
P_d	discharge pressure
P_{HP}	measured discharge pressure
P_i	inlet pressure
P_{LP}	measured pressure downstream of pressure control valve
Q_d	instantaneous volumetric flow-rate across the discharge check-valve for a single piston
$\bar{Q}_d$	average ideal flow rate exiting the pump at the discharge port
Q_{HP}	measured discharge flow rate
Q_i	instantaneous volumetric flow-rate across the inlet check-valve for a single piston
$\bar{Q}_i$	average ideal flow-rate entering the pump at the inlet port
Q_{LP}	measured flow rate downstream of pressure control valve
T	ideal torque required to drive a single piston
$\bar{T}$	average ideal-torque exerted on the pump shaft
V	instantaneous volume of a single piston chamber
V_p	apparent volumetric displacement of the pump
V_t	volume of single piston chamber at when the piston is located at top-dead-center
v	upward velocity of a single piston
x	nondimensional commanded displacement of the pump
α	fluid coefficient of thermal expansion
β	fluid bulk-modulus of elasticity
ΔV	swept volume of a single piston chamber
η	overall pump efficiency
η_m	mechanical pump efficiency
η_v	volumetric pump efficiency
Θ	fluid temperature
θ	angular position of the pump shaft
μ	absolute fluid viscosity
ρ	fluid density
ω	angular velocity of the pump shaft

INTRODUCTION

Background. For the past seventy-five years, the swash-plate type, variable displacement pump has been used in applications where variable pump flow is needed. However, limits have been reached concerning the control and efficiency

of these machines [1,2]. Traditional hydromechanical control systems are giving way to electronic controls in pursuit of greater performance and efficiency. Today's electrohydraulic pump controls typically consist of solenoid coil actuators and sensors for measuring fluid pressure and swash plate position. Yet the basic pump design principles, along with the efficiency and dynamic response, remain unchanged. New digital fluid power technology embodies digital design principles within the fluid domain and a deeper integration of electrical components. There are multiple ongoing efforts to develop digital hydraulic pumps and motors. One notable example is the check-valve type digital displacement pump developed by Artemis Intelligent Power Ltd (Artemis). This machine is now being offered as a commercial product, the first of its kind, and boasts a faster response rate and a higher efficiency than the traditional swash-plate type machines. Various designs for digital hydraulic pumps are extant in patents and academic publications. For the sake of clarity in the present work, "digital displacement" refers to technology developed by Artemis. The distinction seems appropriate since Artemis coined the term and holds trademark rights to its use for commercial purposes.

At the present time, calculating the overall efficiency of the digital displacement pump is straightforward as the input power and the output power of this machine is easily measured. However, calculating the volumetric and mechanical efficiencies for this machine is more difficult. This difficulty arises from a known feature of the digital displacement pump where the apparent volumetric displacement of the machine decreases with pressure. This reduced displacement is observable from both an input power and an output power perspective and is therefore not a power loss – it is an apparent reduction in displacement, or as some would say it is a phenomenon of pump shrinkage. Previous work has been conducted to quantify the reduction in the ideal volumetric displacement for the digital displacement pump as pressures increase [3] In this present paper, this analysis is used with experimental data to illustrate a method for calculating and plotting the volumetric and the mechanical efficiencies of the digital displacement pump.

Literature Review. Digital fluid power lacks a precise definition, referring to a variety of hydraulic and pneumatic systems with discrete states. One area of digital hydraulics includes fluid systems that are analogous to electrical power systems. The earliest digital pump of this type known to the authors was developed by Republic Aviation for the US Air Force in 1964 [4]. It was a pulsating flow generator analogous to an alternating current electrical generator. Other research involving the dynamics of pulse-width modulated (PWM), solenoid-actuated valves was first published in 1984 [5]. This work and others like it focused on dynamic response, component design and hydraulic-electronic interface; the energy efficiency of the system was not a primary consideration [6,7]. In 2003, Scheidl and Hametner published an important result that showed that the operating efficiency for a PWM valve was dependent upon the switching frequency of the pulse [8], leading one to consider the idea that the efficiency may be dependent in on the duty-ratio of the valve. In 2005, authors from the University of Minnesota proposed a way to create a variable flow rate from a fixed displacement pump with a PWM valve and an accumulator. The authors claimed improved efficiency of the system compared to systems with a constant pump flow rate [9,10]. Other authors contributed to the study of virtually variable displacement pumps based on PWM switching [11-13]. The switching time of modern hydraulic valves (typically >1 ms) is much slower than the transistors in PWM electrical systems, which continues to be a challenging frontier in this area of research.

Another approach to digital hydraulic pumps is actively controlling individual pistons within a piston pump, thereby dividing the flow output into discrete steps or pulses. The piston control valves may also have discrete on-off states. Research in this direction was first published in 1984 by Salter and Rea [14] from the University of Edinburgh wherein the conceptual design of a digital displacement pump was proposed. Continued research resulted in patent applications in 1989 and 1990 and a PhD thesis by Rampen in 1992 with measurements from a working prototype [15-17]. The researchers in Edinburgh formed Artemis as a technology start-up company in 1994 and continued to develop the technology. Partnerships with established manufacturers including Danfoss resulted in many more patents and publications in the last 25 years. Digital displacement pump/motor technology has been successfully demonstrated in applications including wind power, rail, passenger vehicles and off-highway machinery.

In the last 10 years or so, academic interest in innovative hydraulic pump designs has increased. Research is ongoing at multiple universities in Europe and North America, which was partly summarized in a review paper by Linjama [18]. An annual conference on digital fluid power is held at European universities since 2008, most recently in Aalborg, Denmark. Other academic conferences around fluid power technology regularly include papers about digital pump design which are too numerous to cite here.

There is an international standard method for experimentally determining the volumetric displacement of hydraulic pumps used for fluid power transmission [19]. In this method, the displacement of a pump or motor is calculated from measured speed and flow rate over a range of outlet pressures. The derived (or ideal) displacement is then determined by extrapolating the measured points to zero pressure. Other methods exist for determining volumetric displacement which can be found in textbooks and scholarly papers. In any case, a pump's volumetric displacement is defined to be constant with respect to pressure. Such methods are well-suited for common hydraulic pumps and motors, including axial piston and gear type machines. Digital displacement pumps use a radial piston configuration with check valves for flow control. Experience with check valve pumps has shown that the apparent displacement of the pump tends to shrink as the discharge pressure increases. That is, the input torque and the output flow rate at high pressure are both lower than would be expected if displacement was constant. This phenomenon of pump displacement shrinkage is known to pump designers to be related

to fluid compressibility. In the academic literature, fluid compressibility effects have typically been considered as volumetric losses. For example, Johnston modeled a check valve piston pump, noted displacement shrinkage in simulated and measured results and considered it a reduction in volumetric efficiency (i.e. a flow loss) [20]. However, for check valve pumps, the apparent shrinkage is not due to energy loss as made evident by the fact that both the input and output power of the machine show the same reduction in apparent displacement. While the literature illustrates a growing trend toward digital hydraulics and check valve type pumps [21-25], their theoretical characteristics are worthy of further study.

Caldwell was the first author to publish a mathematical model of volumetric displacement for check valve pumps which explicitly considers displacement shrinkage due to fluid compressibility [26]. He noted the need to separate the effects of leakage and compressibility, both of which reduce the output flow. He then created a semi-empirical loss model based on steady-state pump measurements. Once torque and flow losses are known, equations for the ideal or apparent volumetric displacement as well as volumetric and mechanical efficiency are readily derived. The authors of this current paper have recently conducted a rigorous analysis of the ideal input and output power of the digital displacement pump, and have developed closed-form expressions illustrating the physical mechanisms and magnitude of displacement shrinkage [3]. The focus of this present work is to employ these closed-form expressions for the purpose of calculating and plotting the volumetric and mechanical efficiencies for a digital displacement machine.

DESCRIPTIONS

A schematic for a single piston of the digital displacement pump is shown in Fig. 1. As shown in this figure, the piston reciprocates in the vertical direction using a cam-follower displacement device. The instantaneous velocity of the piston is shown by the symbol v and the torque, angular speed, and angular displacement of the cam are shown by the symbols T, ω, and θ respectively. It is important to note that an actual pump would be comprised of multiple pumping units depending upon the design choice of the manufacturer. Also, in the analysis which follows the mechanism for displacing the piston does not have to be a cam-follower device. This mechanism could be a slider-crank device or any reciprocating device that produces a cyclic change in volume for the piston chamber. In Fig. 1, the pressure within the piston chamber is shown by the symbol P and the instantaneous volume of fluid within this chamber is given by V. The symbol β is used to represent the fluid bulk modulus-of-elasticity which describes the compressibility of the fluid. Check valves are shown on either side of the piston to facilitate the inlet flow Q_i and the discharge flow Q_d. The inlet and discharge pressures are shown in Fig. 1 using the symbols P_i and P_d. An on-off control valve is shown to bridge the inlet check valve in order to achieve the digital displacement control of the pump described in the subsequent paragraphs.

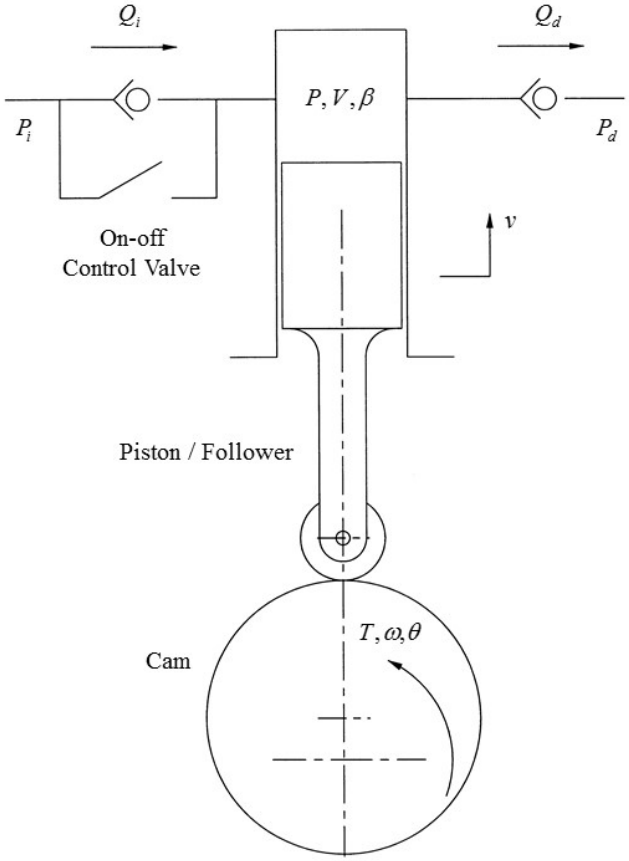

Figure 1. A schematic of a single piston within the digital displacement pump

In Fig. 1 the left-hand-side of the piston chamber is shown to use an on-off control valve (represented as a switch) and a passive check-valve in parallel for connecting or separating the piston chamber from the intake pressure P_i. When the control valve is switched on, the switch is in the closed position and the piston chamber is connecting to the inlet in such a way as to facilitate the inlet flow Q_i while keeping the piston pressure P essentially equal to the inlet pressure P_i. In other words, the on-off control valve provides very little resistance to fluid flow when the switch is in the closed position. When the control valve is switched off, the switch is in the open position and flow into the piston chamber is strictly controlled by the check valve. As long as the piston pressure P remains slightly lower than the inlet pressure P_i the inlet flow Q_i is facilitated by the check valve while keeping the piston pressure P essentially equal to the inlet pressure P_i. On the right-hand-side of the piston chamber a passive check-valve is used for connecting or separating the piston chamber from the discharge pressure P_d. As long as the piston pressure P remains slightly higher than the discharge pressure P_d the discharge flow Q_d is facilitated by the

check valve while keeping the piston pressure P essentially equal to the discharge pressure P_d. The proper staging of the on-off control valve is used to adjust the amount of fluid that is pumped across the discharge check-valve, thereby adjusting the commanded volumetric displacement of the machine.

The operation of each piston consists of five stages: control, compression, discharge, expansion and suction. During the first stage of pump operation, the piston is located at bottom-dead-center which is defined as a location where the fluid volume in the piston chamber is at a maximum value. While in this location, the on-off control valve is in the closed position in order to connect the piston chamber to the inlet side of the pump. In this condition, the piston pressure is essentially equal to the inlet pressure. As the piston moves up, the displaced volume of fluid in the piston chamber is pushed *out* of the inlet side of the pump, creating a negative flow rate for Q_i. The important thing to notice is that the displaced fluid does *not* pass into the discharge port since the piston pressure is much lower than the discharge pressure and the discharge check-valve is closed. In other words, the displaced fluid in the piston chamber during this first stage of pump operation does not contribute to the average discharge flow-rate of the pump, which illustrates the controlled effort to reduce the apparent volumetric displacement of the machine.

At the beginning of the second stage of pump operation, the on-off control valve has just been opened to disconnect the piston chamber from the inlet side of the pump. During this stage the piston continues to advance into the piston chamber while increasing the piston pressure above the inlet pressure, but not having yet raised the pressure to the level of the discharge pressure. In other words, this stage of pump operation is carried out while both check valves are closed and the fluid within the piston chamber is being compressed. When the pressure in the piston chamber reaches the discharge pressure of the pump, this second stage of pump operation is finished. Once again, it is important to note that no flow has been delivered to the discharge side of the pump during the compression stage of pump operation. In other words, similar to the first stage, the displaced fluid in the chamber during the compression stage does not contribute to the average discharge flow-rate of the pump, which again reduces the apparent volumetric displacement of the machine.

At the beginning of the third stage of pump operation, the discharge check-valve has just been opened to connect the piston chamber to the discharge side of the pump. During this stage, the piston continues to advance into the piston chamber thus pushing fluid across the discharge check-valve of the pump. Obviously, this is the operating stage where the displacement of the pump contributes to the discharge flow, thus producing the apparent volumetric displacement of the machine.

At the beginning of the fourth stage of pump operation the piston is located at top-dead-center. As the shaft continues to rotate and the piston begins to retract from the piston chamber, the volume in the piston chamber expands and the fluid pressure begins to drop. Since the fluid pressure remains between the discharge and inlet pressures of the pump, the check valves on both sides of the pump are closed and no fluid exits or enters the machine. This stage of pump operation reduces the amount of fluid drawn into the pump from the inlet side. Furthermore, the relaxation of the pressurized fluid during this stage is used to *assist* the torque on the input shaft in the direction of pump rotation, thus recapturing some of the energy that was used to compress the fluid during the compression stage of pump operation.

At the beginning of the final stage of pump operation, the expansion stage has been completed and the fluid pressure within the piston chamber is now equal to the inlet pressure of the pump. Under these conditions a positive volumetric flow rate Q_i enters the pump and the piston chamber fills with fluid in preparation for a new pumping cycle.

IDEAL TORQUE AND FLOW

As previously mentioned, a rigorous analysis of the ideal shaft torque, and the ideal discharge flow for the pump has been conducted in Ref. [3]. As an ideal analysis, the results of this study do not include internal friction or fluid leakage; but they do include the compressibility effects that were described in the Descriptions section of this paper. In summary of this work, the average ideal-torque exerted on the input shaft of the pump is given by

$$\overline{T} = \left[x - \left(x + \frac{V_t}{\Delta V} \right) \left(\frac{(P_d - P_i)}{\beta} \right) \right] \frac{N \Delta V}{2\pi} (P_d - P_i) \quad , \quad (1)$$

and the average ideal discharge-flow of the pump is given by

$$\overline{Q}_d = \left[x - \left(x + \frac{V_t}{\Delta V} \right) \left(\frac{(P_d - P_i)}{\beta} \right) \right] \frac{N \Delta V}{2\pi} \omega \quad . \quad (2)$$

In these results x is the nondimensional commanded displacement of the pump which can vary between zero and unity. This quantity depends upon the amount of time that the digital valve remains open. The symbol V_t describes the fluid volume in the piston chamber when the piston is located at top-dead-center, ΔV is the mechanical stroke volume for a single piston chamber, N is the number of pistons in the pump design, and all other symbols have been previously defined.

By inspection it can be seen that in the absence of compressibility effects, Eqs. (1) and (2) reduce to the standard form for the ideal torque and the ideal discharge-flow for a positive displacement pump. It is also useful to observe that the terms within the square brackets of Eqs. (1) and (2) are identical. In other words, the square-bracketed terms in these two equations – one input equation and one output equation – describes the physical cause for the apparent shrinkage in pump displacement as pump pressure increases. This shrinkage is not associated with a power loss as the both the input power and the output power shrink at the same rate.

APPARENT VOLUMETRIC DISPLACEMENT AND EFFICIENCY CALCULATIONS

By inspecting either Eq. (1) or Eq. (2) it may be observed that the apparent volumetric displacement of the pump per unit radian is given by

$$V_p = \left[x - \left(x + \frac{V_t}{\Delta V} \right) \left(\frac{(P_d - P_i)}{\beta} \right) \right] \frac{N \Delta V}{2\pi} \quad . \tag{3}$$

Because the pumping pistons are each controlled independently, the same average discharge flow rate may be obtained with a variety of control algorithms. For example, $x < 1$ implies a *part stroke* algorithm. Flow rate is reduced by disconnecting the cylinder from the low pressure source while the pistons are mid-stroke, as was explained previously. Alternately, flow rate may be reduced by using fewer pistons which pump through full strokes. For a *full stroke* control algorithm, $x = 1$ and N is replaced by a lesser number. As shown in Eq. (3), the apparent volumetric displacement of the pump is reduced as pressures increase due to the compressibility of the fluid. This feature is enhanced by having a large volume of fluid near top-dead-center as shown by the symbol V_t. If the compressibility effects are neglected for the pump, Eq. (3) may be modified to describe the volumetric displacement of the machine as

$$V_p = x \frac{N \Delta V}{2\pi} \quad . \tag{4}$$

Using well accepted definitions for efficiency, the overall efficiency for the digital displacement pump is given by

$$\eta = \frac{(P_d - P_i)\, \bar{Q}_d}{\bar{T}\, \omega} = \eta_v \times \eta_m \tag{5}$$

where the volumetric and mechanical efficiencies are given respectively as

$$\eta_v = \frac{\bar{Q}_d}{V_p\, \omega} \quad \text{and} \quad \eta_m = \frac{V_p (P_d - P_i)}{\bar{T}} \quad . \tag{6}$$

In these equations, the volumetric displacement V_p is given in either Eq. (3) or Eq. (4) depending on whether or not the compressibility effects are included. From these expressions it may be seen that the volumetric displacement does not alter the overall efficiency calculation; however, it has a significant impact on determining the volumetric and mechanical efficiencies. In the following sections it will be shown that without accounting for the apparent displacement that changes with increased pressure, the volumetric and mechanical efficiency calculations are incorrect and sometimes unrealistic.

EXPERIMENTS

The efficiency characteristics of a digital displacement pump were evaluated experimentally. Pump efficiency tests were conducted at the Danfoss facility in Ames, Iowa, USA in accordance with internal and international standards [27]. The measured pump was an E-dyn® 96 cc/rev radial piston machine supplied by Artemis. Photographs of the pump and test stand are shown in Fig. 2.

Figure 2. Photos of the experimental equipment

Figure 3 shows a simplified schematic diagram of the hydraulic circuit. Since the test stand can be configured for a variety of tests, there is an assortment of check valves, ball valves, relief valves and lines which have been omitted from the diagram for the sake of clarity. The reader may notice that there is no pump case drain line. The pump does not have an external

drain; leakage past the pistons returns to the inlet internally. Typically, pump discharge flow rate is measured either upstream or downstream of the pressure control valve. In the present experiment, the discharge flow rate was measured in both locations simultaneously, labeled high and low system pressure in the diagram. An *in situ* measurement of fluid bulk modulus is possible with the two flow meters. Instrument descriptions and accuracy are shown in Table 1.

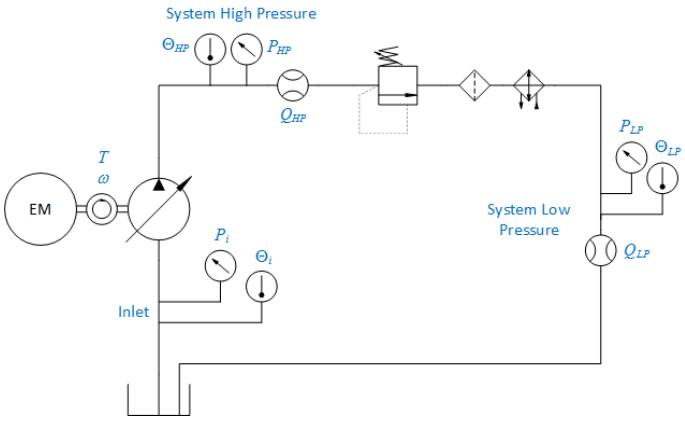

Figure 3. Simplified schematic of the experimental circuit

Table 1. Instruments and their properties

Measured Quantity	Sensor Type	Sensor Description	Sensor Accuracy
Shaft speed	Optical encoder	Himmelstein MCRT 84704	60 pulses per revolution
Shaft torque	Non-contact digital torque meter	Himmelstein MCRT 84704, 1130 Nm full scale	±0.036% of full scale
Pressure, system HP	Strain gauge	Viatran 248, 10000 psi	±0.15% of measured value
Pressure, system LP	Strain gauge	Viatran 248, 10000 psi	±0.15% of measured value
Pressure, inlet	Strain gauge	Viatran 248, 100 psi	±0.15% of measured value
Temperature, all	T-type thermocouple		±1.0 deg C
Flow rate, system HP	Positive displacement, helical	VSE RS 400	±0.5% of measured value
Flow rate, system LP	Positive displacement, helical	Max Machinery 242-261 with 294 transmitter	±0.2% of measured value

Measurements were taken at steady state operating conditions, as listed in Table 2. The test fluid was Shell Tellus 46 hydraulic oil; kinematic viscosity is 30 cSt and 11 cSt at 50° and 80° Celsius respectively.

Table 2. Experimental operating conditions

Quantity	Unit	Value
Speed	rev/min	500, 1000, 1500, 2000, 2500, 2800, 3000
Outlet Pressure	bar	20, 50, 100, 200, 300, 420
Commanded Displacement	%	10, 20, 30, 40, 50, 60, 70, 80, 90, 100
Temperature	°C	50, 80
Pump Flow Control Algorithm		Full stroke, variable part stroke

As explained in the previous section, it is essential to know the fluid bulk modulus in order to properly calculate volumetric and mechanical efficiencies. Measuring the volumetric flow rates at high and low pressure makes it possible to determine the bulk modulus while the pump is in operation. A mass balance equation for the system is given by

$$\rho_{HP}\, Q_{HP} = \rho_{LP}\, Q_{LP} \tag{7}$$

where ρ_{HP} and ρ_{LP} are the fluid densities at high and low pressure respectively, and Q_{HP} and Q_{LP} are the volumetric flow rates at high and low pressure. A linear equation of state may be used to describe the fluid density as

$$\rho = \rho_o \left[1 + \frac{(P - P_o)}{\beta} - \alpha\,(\Theta - \Theta_o) \right] \tag{8}$$

where the subscript "*o*" identifies a reference condition, ρ is the fluid density at either the high or low pressure, P is either the high or low fluid pressure, Θ is either the high or low fluid temperature, β is the fluid bulk modulus, and α is the coefficient of thermal expansion for the fluid. Using Eq. (8) with Eq. (7), the fluid bulk modulus may be described using experimental data as follows:

$$\beta = \frac{(P_{HP} - P_o)\dfrac{Q_{HP}}{Q_{LP}} - (P_{LP} - P_o)}{\left[1 - \alpha\,(\Theta_{LP} - \Theta_o)\right] - \left[1 - \alpha\,(\Theta_{HP} - \Theta_o)\right]\dfrac{Q_{HP}}{Q_{LP}}} \quad . \tag{9}$$

This equation was used to compute the fluid bulk modulus for this work. In our research, values for the bulk modulus ranged from 13.0 kbar to 13.7 kbar between low and high pressure operation.

RESULTS AND DISCUSSION

One of the most interesting features of the check-valve type, digital displacement pump is that it undergoes an apparent shrinkage in volumetric displacement as the pressure increases. A theoretical explanation for this has been provided in Ref. [3] and presented in Eqs. (1) and (2)where fluid compressibility has been shown to decrease the apparent volumetric displacement of the pump from both an input and an output perspective. In other words, this reduction in displacement is realized by both the input torque and the discharge flow of the machine. Our readers are not surprised by the reduction in discharge flow due to compressibility effects, as this phenomenon is well known and always included in pump efficiency modeling [1,20]. What may be surprising to our readers is that the apparent volumetric displacement of the pump is also reduced from the perspective of the input terminal, which results in a lower torque input than one might ordinarily expect. In fact, this reduction is identical from the perspective of the input and output of the machine, which means there is no energy loss associated with pump shrinkage due to the compressibility of fluid.

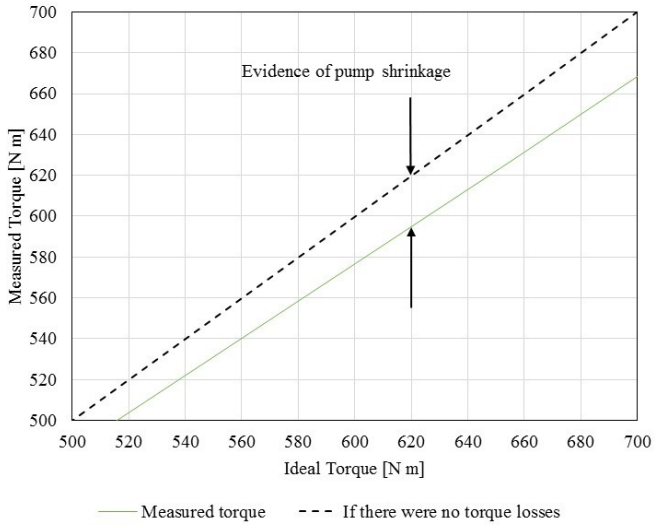

Figure 4. Experimental evidence of pump shrinkage being realized by the input shaft of the machine. For this data, the shaft speed was 1,500 rpm and full pump displacement was being commanded by the control algorithm where $N=12$ and $x=1$.

Figure 4 shows the experimental evidence for pump shrinkage being realized at the input shaft of the machine. In this figure, the measured torque at the input shaft is plotted against the ideal torque as computed using the pressure drop across the pump and Eq. (4) with $N=12$ for this pump design, and $x=1$. If there were no pump shrinkage and there were torque losses due to internal friction of the machine, the measured torque values would have been *above* the 45 degree dashed line in Fig. 4. However, Fig. 4 shows that all measured torque values are *below* the dashed line even when real friction exists within the machine. In other words, the pump shrinkage as realized by the input shaft is more significant than the actual torque loss due to friction. While Fig. 4 describes this phenomenon for a particular operating condition of the machine, it should be noted that pump shrinkage of this type is observable across the entire operating spectrum and is more pronounced as pressures increase.

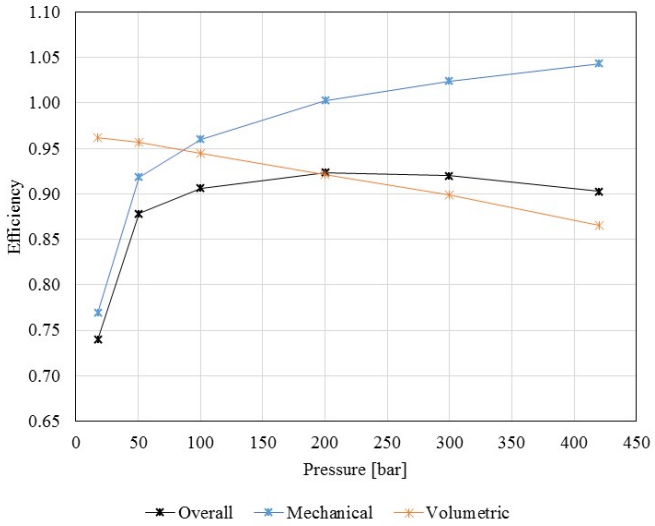

Figure 5. Efficiency plots generated using a *full stroke* algorithm where $x=1$ and $N=0.9\times12=10.8$, and the operating temperatures were 50 degrees Celsius. For these results, Eq. (4) was used to compute mechanical and volumetric efficiencies. Mechanical efficiencies greater than unity, and volumetric efficiencies less than the overall efficiency are unrealistic.

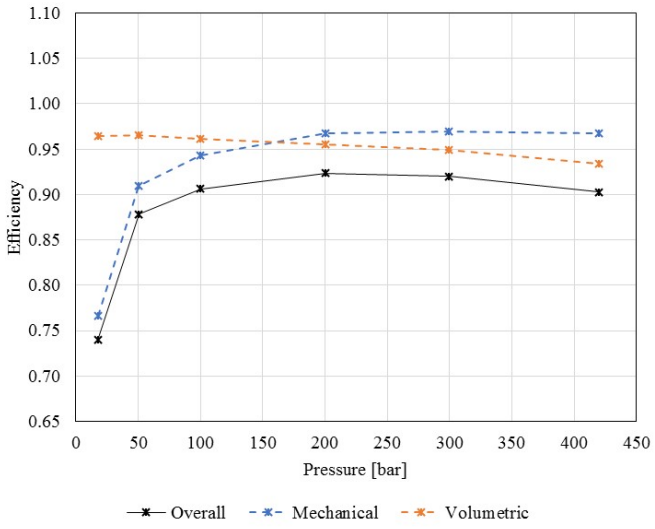

Figure 6. Efficiency plots generated using a *full stroke* algorithm where $x=1$ and $N=0.9\times12=10.8$, and the operating temperatures were 50 degrees Celsius. For these results, Eq. (3) was used to compute mechanical and volumetric efficiencies. Mechanical and volumetric efficiencies are now shown to be realistic. This figure should be compared with Fig. 5.

Figures 5 through 8 are experimental efficiency results, and are presented to illustrate the importance of accounting for pump shrinkage when computing the mechanical and volumetric

efficiencies for the machine. Each figure is presented for an operating shaft speed of 1,500 rpm. Figures 5 and 6 are presented for a *full stroke* algorithm where $x = 1$ and $N = 0.9 \times 12 = 10.8$. Figures 7 and 8 are presented for a *part stroke* algorithm where $x = 0.9$ and $N = 12$. Both algorithms are intended to command similar displacements for the pump.

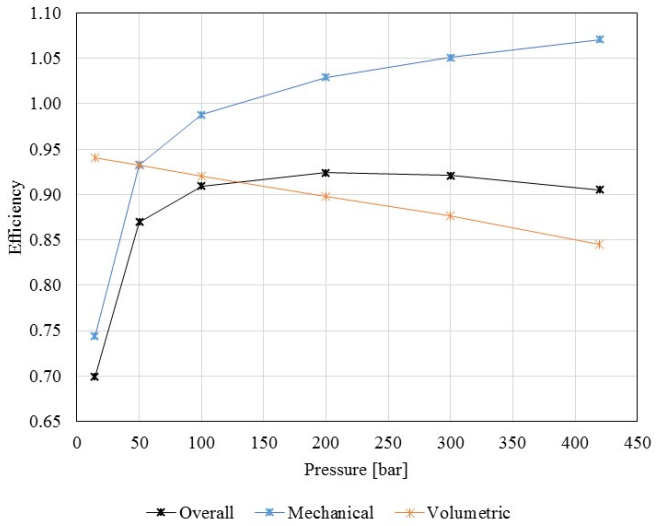

Figure 7. Efficiency plots generated using a *part stroke* algorithm where $x = 0.9$ and $N = 12$, and the operating temperatures were 50 degrees Celsius. For these results, Eq. (4) was used to compute mechanical and volumetric efficiencies. Mechanical efficiencies greater than unity, and volumetric efficiencies less than the overall efficiency are unrealistic.

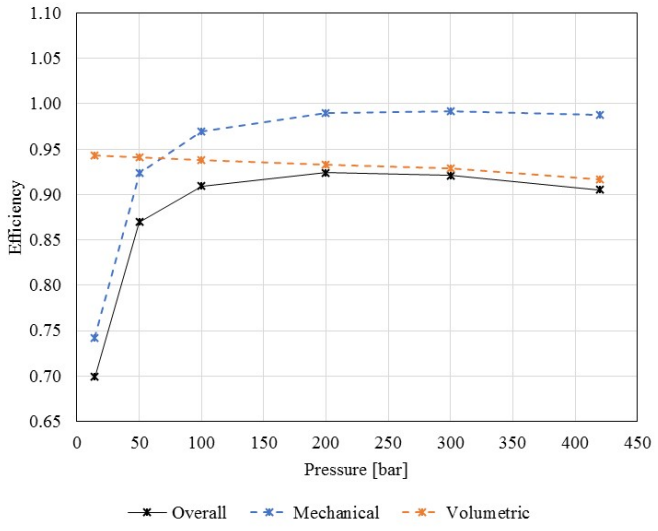

Figure 8. Efficiency plots generated using a *part stroke* algorithm where $x = 0.9$ and $N = 12$ and the operating temperatures were 50 degrees Celsius. For these results, Eq. (3) was used to compute mechanical and volumetric efficiencies. Mechanical and volumetric efficiencies are now shown to be realistic. This figure should be compared with Fig. 7.

As shown in Figs. 5 through 8, the calculations for mechanical and volumetric efficiency that fail to account for pump shrinkage produce unrealistic efficiency results. By failing to account for pump shrinkage, the mechanical efficiency is over estimated and the volumetric efficiency is underestimated by almost 7% at high pressures. See Eq. (6). The calculations that account for pump shrinkage produce results that are realistic.

A comparison of Figs. 6 and 8 shows that the overall efficiency for a machine being controlled by the *full stroke* and *part stroke* control algorithm is very similar. However, the mechanical and volumetric efficiency produced by each control algorithm is somewhat different. A comparison of these figures shows that the *part stroke* algorithm produces a mechanical efficiency that is higher than that of the *full stroke* algorithm, while the volumetric efficiency is lower for the *part stroke* algorithm compared to the *full stroke* algorithm. This result is solely an effect of the control algorithm, not a feature of the calculation method for pump shrinkage or the apparent volumetric displacement of the machine.

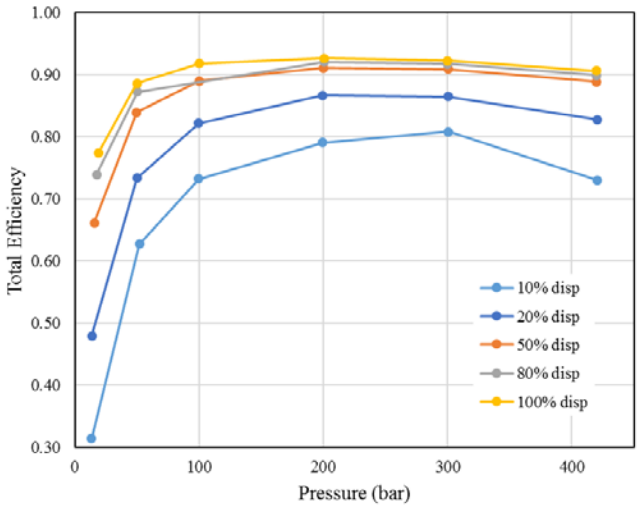

Figure 9. Total efficiency with *full stroke* algorithm and displacement fraction 0.1 to 1.0 at 1500 rpm and 30 cSt fluid viscosity.

The efficiency difference between the two algorithms at partial displacement is primarily due to the number of pistons in use. The *part stroke* algorithm pressurizes all the pistons, resulting in higher leakage and lower friction, while the *full stroke* algorithm only pressurizes the minimum number of pistons required to satisfy the commanded volumetric displacement. With the *full stroke* algorithm, some displacement fractions can be achieved with integer values of *N*. For example, *N* = 9 gives 9/12 = 0.75 displacement fraction. Nine pistons are active and 3 are idle during every revolution. *N* can also have non-integer values, such as *N* = 9.5. Then the displacement

fraction is 9.5/12 = 19/24 = 0.792. Nine pistons are active during the first revolution, and 10 pistons are active during the second revolution, always with full strokes (x = 1). The desired displacement fraction is satisfied as a time average of full piston strokes. The full stroke algorithm is analogous to an analog-to-digital converter. An analog value (desired displacement fraction) is converted to a sequence of ones and zeros (on and off pistons). Any analog value can be converted to a sufficiently long binary sequence. In practice, a reasonable compromise can be found between the resolution of the desired flow rate and the maximum length of the piston control sequence.

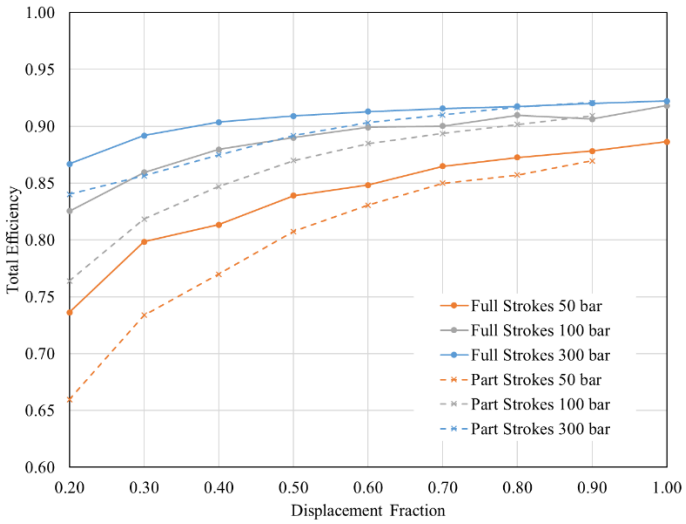

Figure 10. Efficiency plots comparing *full stroke* and *part stroke* flow algorithms

The difference between full and part stroke algorithms in terms of total efficiency becomes more pronounced with decreasing displacement, as shown in Fig. 10. This figure highlights the original motivation for the digital displacement design, which is to reduce power losses at partial displacement by pressurizing only the minimum number of pistons [14].

CONCLUSIONS

The following conclusions are supported by the analysis, results and discussion of this paper:

1. That the compressibility effects within the pump reduce the apparent volumetric displacement of the machine. This reduction is not accompanied with an energy loss since the input torque and the discharge flow are reduced by the same percentage.
2. That without accounting for the apparent pump shrinkage, computations of the volumetric and mechanical efficiencies are unrealistic with a mechanical efficiency that often exceeds unity and a volumetric efficiency that is less than the overall efficiency.
3. That by accounting for the apparent pump shrinkage according to Eq. (3) the correct volumetric and mechanical efficiencies may be computed, and that these often differ from the uncorrected results by as much a 7%.
4. That the mechanical and volumetric efficiencies for the pump depend upon whether or not the *full stroke* or *part stroke* algorithm is being used to control the displacement. The *part stroke* algorithm produces a higher mechanical efficiency and a lower volumetric efficiency for the pump, compared to the *full stroke* control algorithm.

While seeking to take advantage of the high efficiencies that are typical of a check-valve type, digital displacement pump, the conclusions of this research are useful for serving an industry that is accustomed to considering the volumetric and mechanical efficiencies of these machines.

ACKNOWLEGEMENTS

Thanks to Curtis Hansen, Tim Huxford and Bennett Torrance for their assistance with the experiments.

REFERENCES

[1] Manring, N.D. 2016. Mapping the efficiency of a hydrostatic transmission. ASME Journal of Dynamic Systems, Measurement, and Control. 138:031004-1-8.

[2] Manring, N.D., and V. Mehta. 2011. Physical limitations for the bandwidth frequency of a pressure controlled, axial-piston pump. ASME Journal of Dynamic Systems, Measurement, and Control. 133:1-12.

[3] Manring, N.D., and C. Williamson. (under review). The theoretical displacement of a check valve type, digital displacement pump. ASME Journal of Dynamic Systems, Measurement, and Control.

[4] Republic Aviation Corporation. May 1964. Research Investigation of Hydraulic Pulsation Concepts. US Air Force Contract AF33 (657)-10622. Unclassified. Wright-Patterson Air Force Base, Ohio.

[5] Tanaka, Hirohisa., Hiroyoshi Tanaka, and A. Kazuo. October 1984. Electro-hydraulic digital control of 3-way on/off solenoid valves. Transactions of the Japan Society of Mechanical Engineers, Part B. Volume 50, Issue 458. Pp. 2663-2666. ISSN: 03875016

[6] Muto, T., H. Yamada, and Y. Suematsu. 1990. PWM-digital control of a hydraulic actuator utilizing two-way solenoid valves. Journal of Fluid Control. Vol. 20. Issue 2. Pp. 24-41. ISSN: 8755-8564

[7] Suematsu, Y., H. Yamada, T. Tsukamoto, and T. Muto. 1993. Digital control of electrohydraulic servo systems operated by differential pulse width modulation. Japan Society of Mechanical Engineers, International Journal. Series C, Vol. 36, No. 1. Pp. 61-68.

[8] Scheidl, R., and G. Hametner. 2003. The role of resonance in elementary hydraulic switching control. Proceedings of the Institution of Mechanical Engineers. Part I, 217(6), pp. 469-80.

[9] Li, P., C. Li, and T. Chase. 2005. Software enabled variable

displacement pumps. Proceedings of the 2005 ASME-IMECE Conference. Paper No. IMECE2005-81376.
[10] Rannow, M.B., H.C. Tu, P. Li, and T. Chase. 2006. Software enabled variable displacement pumps – experimental studies. Proceedings of the 2006 ASME IMECE Conference. Paper No. IMECE2006-14973.
[11] Nieling, M., M.J. Fronczak, and N.H. Beachley. 2005. Design of a virtually variable displacement pump/motor. Proceedings of the 50th National Conference on Fluid Power, Las Vegas, Nevada USA. pp. 323-336.
[12] Lumkes, J., M. Batdorff, and J. Mahrenholz. 2009. Model Development and Experimental Analysis of a Virtually Variable Displacement Pump System. International Journal of Fluid Power. Vol. 10. Issue 3, pp. 17-27.
[13] Feng, W., G. Linyi, C. Jianwei, and C. Ying. 2007. Research on deep-sea electric power generation technique from seawater pressure. Proceedings of the 2007 ASME IMECE Conference. Paper No. IMECE2007-41694.
[14] Salter, S.H., and M. Rea. 1984. Hydraulics for wind. European Wind Energy Conference. Hamberg, Germany.
[15] Salter, S.H., and W.H.S. Rampen. 1989. Pump control method and poppet valve therefore. Patent No. EP0361927 A1.
[16] Salter, S.H., and W.H.S. Rampen, 1990. Improved fluid working machine. Patent No. EP0494236 B1.
[17] Rampen, W.H.S., 1992. The Digital Displacement Hydraulic Piston Pump. Ph.D. Thesis. University of Edinburgh. Edinburgh, United Kingdom.
[18] Linjama, M. Digital Fluid Power – State of the Art. 2011. Proceedings of the Twelfth Scandinavian International Conference on Fluid Power, Tampere, Finland.
[19] ISO 8426:2008. Hydraulic fluid power – Positive displacement pumps and motors – Determination of derived capacity.
[20] Johnston, D.N. 1991. Numerical modelling of reciprocating pumps with self-acting valves. Proceedings of the Institution of Mechanical Engineers. Vol 205, pp. 87-96.
[21] Pan, M., N. Johnston, J. Robertson, A. Plummer, A. Hillis, and H. Yang. 2015. Experimental Investigation of a switched inertance hydraulic system with a high-speed rotary valve. Journal of Dynamic Systems, Measurement, and Control. Vol. 137. 121003-1-9.
[22] Wisch, J.K., N.D. Manring, and R.C. Fales. 2017. Dynamic characteristics of a pressure-compensated inlet-metered pump. Journal of Dynamic Systems, Measurement and Control. Vol. 139. 064501-1-6.
[23] Leati, E., R. Scheidl, and A. Ploeckinger. 2013. On the dynamic behavior of check valves for high frequency oscillation pumps. Proceedings of the ASME/BATH 2013 Symposium on Fluid Power and Motion Control, FPMC2013-4416, pp. 1-10.
[24] He, X., B. Zhu, Y. Liu, and Z. Jiang. 2011. Study on a seawater hydraulic piston pump with check valves for underwater tools. Proceedings of the IMechE, Vol. 226 Part A: Journal of Power and Energy, pp. 151-160.
[25] He, X., W. Huang, B. Zhu, and L. Luo. 2011. Air suction characteristics of a water hydraulic piston pump with check valves. Journal of Fluids Engineering. Vol 133. 114502-1-3.
[26] Caldwell, N.J. 2007. Digital displacement hydrostatic transmission systems. Ph.D. Dissertation. University of Edinburgh. Edinburgh, United Kingdom.
[27] Manring, N. D. 2005. Hydraulic Control Systems. John Wiley & Sons. New York. ISBN 978-0-471-69311-6.
[28] ISO 4409:2007. Hydraulic fluid power — Positive-displacement pumps, motors and integral transmissions — Methods of testing and presenting basic steady state performance.